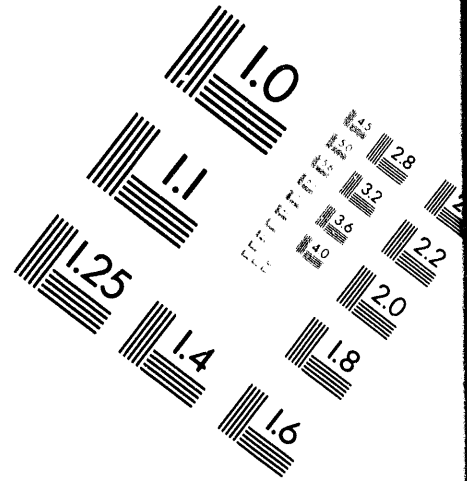
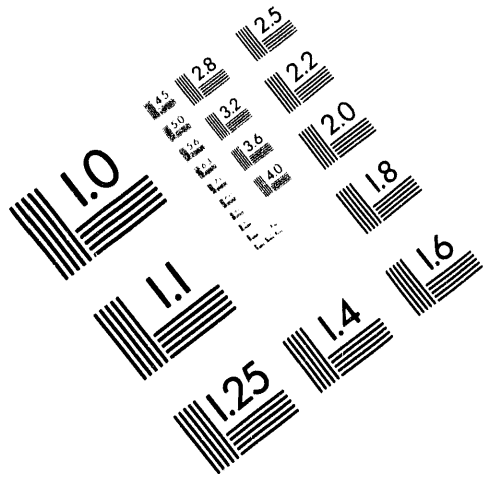




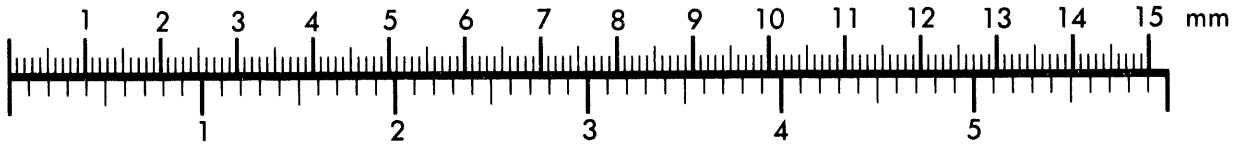
AIM

Association for Information and Image Management

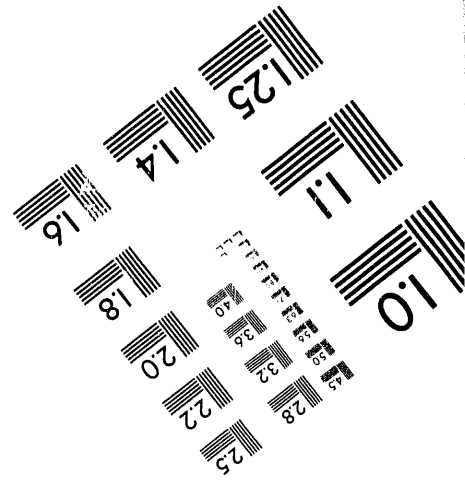
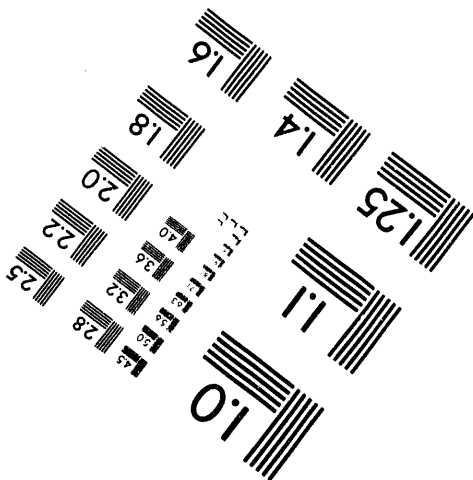
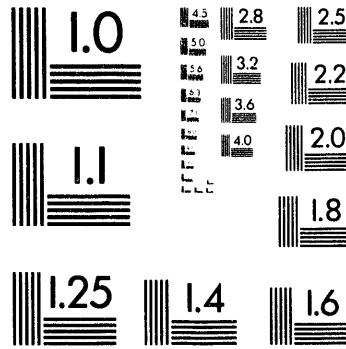
1100 Wayne Avenue, Suite 1100
Silver Spring, Maryland 20910
301/587-8202



Centimeter



Inches



MANUFACTURED TO AIM STANDARDS
BY APPLIED IMAGE, INC.

1 of 1

Fast Electrons, Filamented Laser Light, and the Fast Ignitor

W. L. Kruer and S. C. Wilks

L-472, Lawrence Livermore National Laboratory, Livermore, CA 94550

We report on the absorption of laser energy that results when an ultra-intense laser pulse is incident onto a sharp vacuum-plasma boundary, where the initial shelf density of the plasma is much greater than the critical density, n_{cr} . It is found that 2-D effects greatly increase the amount of absorption into hot electrons, over the amount predicted using 1-D theory. In particular, a scaling for the absorption as a function of density, for a fixed laser intensity, implies that the absorption will be of order 30% for densities well in excess of $100 n_{cr}$. The interaction is studied using both 1- and 2- dimensional particle-in-cell (PIC) simulations. The 1-D results agree quite well with a simple scaling of $J \times B$ heating, where the laser electric field penetrates a skin depth into the overdense plasma and subsequently heats electrons. In 2-D, when the laser is incident at an angle, the absorption is seen to increase substantially due to a form of resonant absorption that occurs in steep density profiles. We find that the inclusion of kinetic and multi-dimensional effects are crucial to obtaining a complete picture of the interaction. The ability of ultra-intense lasers to produce acceptable amounts of hot electrons necessary for the fast ignitor fusion concept will also be assessed.

The main motivation for this work is the fast ignitor fusion concept¹, which employs ultra-high intensity lasers to (1) bore a channel through the corona and then (2) generate hot electrons at the end of this channel. These electrons are then used to heat the highly compressed core. The hole boring laser is roughly 10-100 picoseconds in duration, and has $I\lambda^2 \leq 10^{19} \text{ W } \mu\text{m}^2/\text{cm}^2$. The laser used to generate the hot electrons is roughly 5 picoseconds long, and has $I\lambda^2 \sim 10^{20} \text{ W } \mu\text{m}^2/\text{cm}^2$. The fast ignitor requires a large number of energetic (500 keV-1MeV) electrons. This energy is chosen so that the electron range is approximately equal to the range of a 3.5 MeV alpha particle. Therefore, we are interested in maximizing the laser absorption into hot electrons with the appropriate energies.

Previous 2-D simulations² at low plasma densities ($n \sim 4n_{cr}$) showed good absorption ($A \sim 30\text{-}50\%$) into hot electrons, with a nearly Maxwellian distribution with the temperature approximately given by the ponderomotive potential of the laser. Recent work in 1-D³, using much higher densities ($\sim 100\text{-}300 n_{cr}$), showed a considerable reduction in absorption into hot electrons ($<1\%$), with most of the absorbed energy ($\sim 3\%$) going into the formation of a collisionless ion shock. The goal of this work is to determine if the low

MASTER

EP

amount of absorption into hot electrons in the 1-D simulations is due to the fact that a higher electron density was used, or due to the 1-D geometry, or some combination of the two. To this end, we will first explain the low absorption found in 1-D simulations. We then present results obtained with high density ($n \sim 50-100 n_{cr}$) 2-D simulations.

The particle-in-cell computer code ZOHAR⁴, written by Langdon and Lasinski, was used for all simulations. It should be noted that the equation of motion for the electrons is relativistically correct, and that all resulting nonlinearities are thus included in the simulations. Particles move in the x-y plane. The electric field of the laser is in the plane of particle motion (for 2-D) and this is considered p-polarization: For both the 1-D and 2-D cases, the ions are always mobile with a mass ratio of 1/2000. The 2-D runs are the most realistic representation of the interaction of interest thus far.

In 1-D, JxB heating is the principal mechanism available for energy to be transferred into electrons at a steep vacuum plasma interface where the plasma density is greater than critical.⁵ Briefly, this mechanism can be traced to the ponderomotive force of the laser due to the penetration of the laser electric and magnetic fields a skin depth into the overdense plasma. The non relativistic version of this force can be written as

$$f_{pond} = - \frac{\partial}{\partial x} \left\{ \frac{mv_{osc}^2}{2} \frac{4\omega_0^2}{\omega_{pe}^2} \exp^{-\frac{2\omega_{pe}}{c} x} \left[\frac{1 + \cos 2\omega_0 t}{2} \right] \right\} .$$

Heating is the result of that component of the JxB force that oscillates the electrons at the vacuum-plasma interface with a frequency of twice the laser frequency. The electrons at the boundary oscillate in this "non resonant" wave. The phases of some of the electrons oscillating in this wave may be such that they can escape this oscillation; hence, the electrons are given a non adiabatic kick into the overdense plasma. However, only a fraction of the electrons may escape the wave, and how many escape will depend on the strength of oscillating force. Notice that the magnitude of the force is dependent on ω_0^2/ω_{pe}^2 , or equivalently, n_{cr}/n . Thus, as the electron density increases, the magnitude of the force goes down, and so less energy is transferred to hot electrons. The net result is that the amount of laser light absorbed decreases with increasing density in one dimension. This is consistent with the results of Reference 3, which also found that at these high densities the majority of absorbed laser energy goes into ion motion.

Once a second dimension is added, a number of additional absorption mechanisms become available for heating the electrons. We will concentrate on the following: (1) rippling of the critical surface⁶ (2) resonance absorption in steep density profiles^{7,8,9,10,11} (3) creation of a lower shelf density¹² (3) and relativistic filamentation.^{13,14}

A rippling of the critical surface has long been invoked as a mechanism to explain anomalously high absorption found in intense laser plasma interactions^{15,16}. In fact, this mechanism can strongly affect the absorption, even for interactions at $I\lambda^2 \sim 10^{16} \text{ W } \mu\text{m}^2/\text{cm}^2$ for long pulses (> 1 nanosecond.) For picosecond (and shorter) pulses with low laser intensities, rippling may not occur. The wavelength of the perturbation on the surface is typically on the order of the laser wavelength. Due to surface rippling, the absorption is enhanced, particularly at larger angles, where a larger component of the electric field can drive electrons across the critical surface. When $I\lambda^2 > 10^{16} \text{ W } \mu\text{m}^2/\text{cm}^2$, this effect becomes even more pronounced.

"Not-so-resonant" absorption is a related effect that occurs for obliquely incident, p-polarized light in a sufficiently small density gradient. Briefly, this is a parameter regime where the laser is so intense that the excursion of an electron in the driven wave at the vacuum plasma interface is so large that it is literally pulled out into vacuum, then sent back into the plasma. As with the ponderomotive heating discussed above, some of these particles may be accelerated nonadiabatically back into the plasma, taking some of the laser energy with them, thus causing the laser energy to be absorbed during the interaction. Note that the frequency of this driven wave is now ω_0 , and not $2\omega_0$, as was the case for the JxB heating. This mechanism is quite efficient at absorbing laser energy for oblique incidence. In fact, Brunel showed that the fraction of laser energy absorbed is given by $I_{\text{abs}} = (\eta/2\pi) v_{\text{osc}}(E_L^2/8\pi)$. The dependence of η on the density was found by Kato et al.¹⁰ to be given by $\eta = \alpha/(1 - \omega_0^2/\omega_{pe}^2)$, where $\alpha \approx 1.75$. Notice that this dependence of the absorption on density is much different than that obtained for JxB in 1-D. Finally, it is important to point out that this mechanism is more important than JxB only when the driving field of the electric field (in particular, the component of the E-field that is normal to the surface) is greater than the magnitude of the JxB driving term, i.e., $2E_L \sin\theta > v_{\text{osc}} B_L$, or equivalently $\sin\theta > (v_{\text{osc}}/c) (\omega_0/\omega_{pe})$, as discussed by Denavit in Ref. 3.

The creation of a lower shelf density was observed in the early CO₂ laser experiments¹². This not only allows for increased absorption due to parametric instabilities such as SRS and two plasmon decay to occur in the underdense, but also allows for the possibility of the laser to filament on its way to the critical surface. In fact, for parameters of interest in this paper, the beam can both filament and self-focus, as shown in Fig. 1. Note that not only will the intensity of the laser be higher once it reaches the critical density, but the surface becomes rippled, creating a scenario where enhanced absorption will occur.

Perhaps the most important 2-D absorption mechanism for our purposes is a combination of a rippled surface and Brunel absorption. A sample simulation illustrates the effect. A plane wave is normally incident onto a sharp vacuum plasma interface. Early in

time, the absorption (as expected) agrees with the analogous 1-D result of ~6%. However, as the laser continues to impinge on the interface, the absorption continues to increase until it saturates near 50%. This can be explained by noting that as the interaction proceeds, the surface becomes quite rippled (See Fig. 2). These ripples on the plasma surface allow a component of the electric field of the laser to be oriented across a variation in plasma density. This allows a wave to be driven across the gradient, thus accelerating electrons (some nonadiabatically) that absorb the laser energy. The larger the depth of the ripples become, the more absorption can occur. The ripple could be due to a number of things, for example, a Rayleigh-Taylor instability.¹⁷

An even more important finding is the dependence of the absorption on the initial shelf density. For a given angle of incidence and intensity, the absorption is found to be roughly constant and only weakly dependent on density (for sufficiently large densities.) This can be seen in the simulation results of not-so-resonant absorption presented in Fig. 3. These results are consistent with a number of short pulse experiments, done at somewhat lower intensities^{18,19}. Thus, we now have more confidence in predicting the scaling of the laser absorption with the densities of interest for the fast ignitor, although more work needs to be done in this area.

In conclusion, we have extended the parameter space of simulations done by both our group and J. Denavit on the absorption of ultra-intense lasers at a sharp vacuum-overdense plasma interface. Our previous work was all lower shelf density ($< 10n_{cr}$) work in 2-D. In this report, we reviewed the important findings in 1-D, and presented new simulations done in 2-D with high shelf densities ($25-100n_{cr}$). We examined a number of absorption mechanisms that become available in a two dimensional geometry. We found that the presence of these 2-D effects greatly increases the absorption over that which was predicted from 1-D theory and simulation. In particular, we have shown the dependence of the absorption on the density is characteristic of "not-so-resonant" absorption. This means that although we cannot do simulations at the high densities present in the fast ignitor, we can in principal extrapolate out to these densities. We find the absorption to be constant at ~ 30%, once the density is above $20 n_{cr}$. This implies that it may be possible to generate the large numbers of electrons (in the energy range 500 keV to 1 MeV) necessary to heat the compressed core in the fast ignitor fusion concept.

We would like to acknowledge useful conversations with K. Estabrook, M. Tabak, A. B. Langdon, J. Lindl, M. Rosen, C. B. Darrow, S. Lane, W. B. Mori, and J. M. Dawson. This work was performed under the auspices of the U.S. Department of Energy by Lawrence Livermore National Laboratory under Contract No. W-7405-ENG-48

References

1. M. Tabak, J. Hammer, M. Glinsky, W. L. Kruer, S. C. Wilks, and A. B. Langdon, submitted to *Phys. Rev. Lett.*, (1993)
2. S. C. Wilks, W. L. Kruer, M. Tabak, and A. B. Langdon, *Phys. Rev. Lett.*, **69**,1383 (1992)
3. J. Denavit, *Phys. Rev. Lett.*, **69**,1383 (1992)
4. A. B. Langdon and B. F. Lasinski, *Laser Program Annual Report 1986.*, 2-87 (1986).
5. W. L. Kruer and Kent Estabrook, *Phys. Fluids*, **28**, 430 (1985).
6. J. J. Thomson, W. L. Kruer, A. B. Langdon, C. E. Max, and W. C. Mead, *Phys. Fluids*, **21**, 707 (1978).
7. F. Brunel, *Phys. Fluids*, **31**, 2714 (1988); F. Brunel, *Phys. Rev. Lett.*, **59**, 52 (1987);
8. P. Gibbon and A. Bell, *Phys. Rev. Lett.* **68**, 1535 (1992).
9. K. Estabrook, *Laser Program Annual Report 1986.*, 2-87 (1986).
10. S. Kato, B. Bhattacharyya, A. Nishiguchi, and K. Mima, *Phys. Fluids B*, **5**, 564 (1993).
11. G. Bonnaud, P. Gibbon, J. Kindel, and E. Williams, *Laser Part. Beams* **9**, 339 (1991).
12. Bezzerides, et. al. *Phys. Rev. Lett.* **49**, 202 (1982); R. L. Carman, D. W. Forslund, and J. M. Kindel, *Phys. Rev. Lett.* **46**, 29 (1981).
13. C. E. Max, J. Arons, and A. B. Langdon, *Phys. Rev. Lett.*, **33**, 2091 (1974).
14. W. B. Mori, C. Joshi, J. M. Dawson, D. W. Forslund and J. M. Kindel, *Phys. Rev. Lett.*, **60**, 1298, (1988). A. Borisov, et al., *Phys. Rev. A*, **45**, 5830 (1992).
15. K. Estabrook, et al., *Phys. Rev. Lett.*, **50**, 2082 (1983).
16. Cains et al., *Phys. Rev. Lett.*, **50**, 2082 (1983).
17. E. G. Gamaly, *Phys. Rev. A*, **50**, 2082 (1983).
18. J. C. Kieffer, P. Audebert, M. Chaker, J. P. Matte, H. Pepin, T. W. Johnston, P. Maine, D. Meyerhofer, J. Delettrez, D. Strickland, P. Bado, and G. Mourou, *Phys. Rev. Lett.*, **62**, 760 (1989).
19. U. Teubner, J. Bergmann, B. van Wonterghem, F. P. Schafer, and R. Sauerbrey, *Phys. Rev. Lett.*, **70**, 794 (1993).

Figure Captions

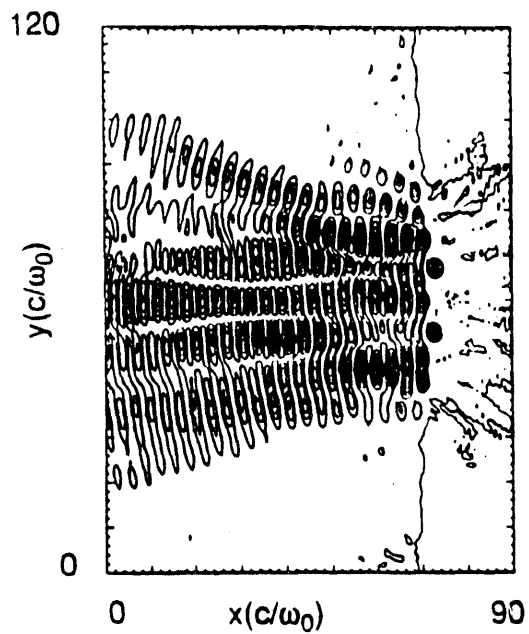
Figure 1. (a) Contour plot of laser intensity ($E^2/8\pi$) in real space (x-y) showing that initially intense (peak intensity $I_0\lambda^2=10^{19} \text{ W } \mu\text{m}^2/\text{cm}^2$), finite spot (FWHM in y dimension is $10\lambda_0$) beam can both filament and self-focus. The plasma density is linearly ramped up from $0.2n_{cr}$ to $0.6n_{cr}$ over the first $70 c/\omega_0$, and rises sharply to $3n_{cr}$ at $70 c/\omega_0$, and stays constant at this density to the end of the simulation box. (b) This leads to a rippling of the critical surface, as shown in the contour plot of electron density in real space.

Figure 2. Contour plots of ion density in real space, for a simulation with parameters $n/n_{cr} = 25$ and plane wave laser with intensity $I_0\lambda^2=10^{19} \text{ W}\cdot\mu\text{m}^2/\text{cm}^2$. (a) Early in time ($\omega_0 t=90$) shows the initially smooth plasma density critical surface. (b) Late time ($\omega_0 t=330$) ion density contours show that a substantial ripple has developed on the surface.

Figure 3. Absorption versus density, showing the scaling that was found in Reference 10. In this series of 2-D simulations, two laser beams (incident at $\pm 45^\circ$) with intensity $I\lambda^2 = 3.4 \times 10^{19} \text{ W}\cdot\mu\text{m}^2/\text{cm}^2$ are shot at an initially steep overdense plasma vacuum interface for a variety of densities. The fact that the absorption levels out at a nonzero value for large densities, is in marked contrast to what was found in 1-D.

Contours of transverse electric field

$$I_{\text{initial}} = 10^{19} \text{ W/cm}^2$$



Contours of plasma density

underdense plasma
(0.2-0.6 n_{cr})

overdense plasma
(3 n_{cr})

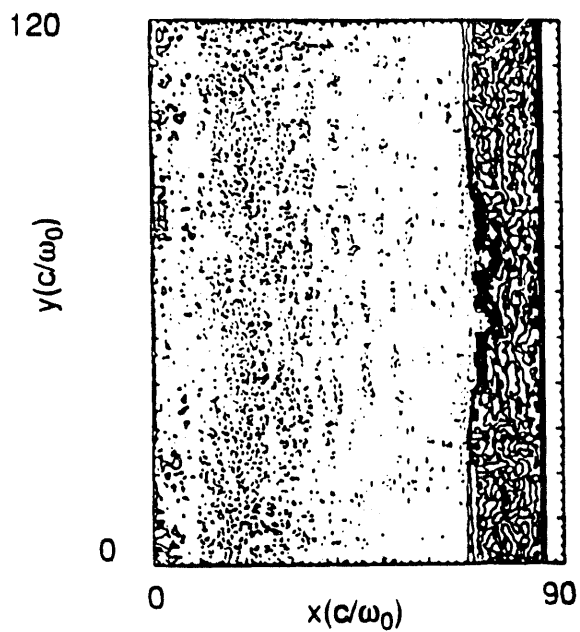


FIG. 1

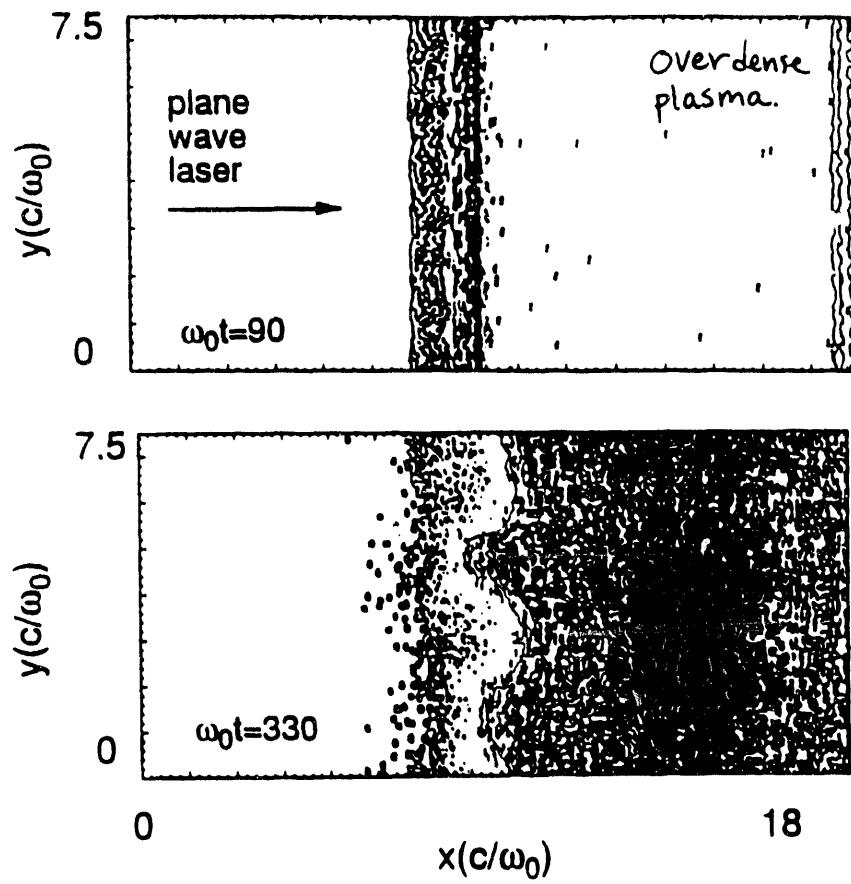


FIG. 2

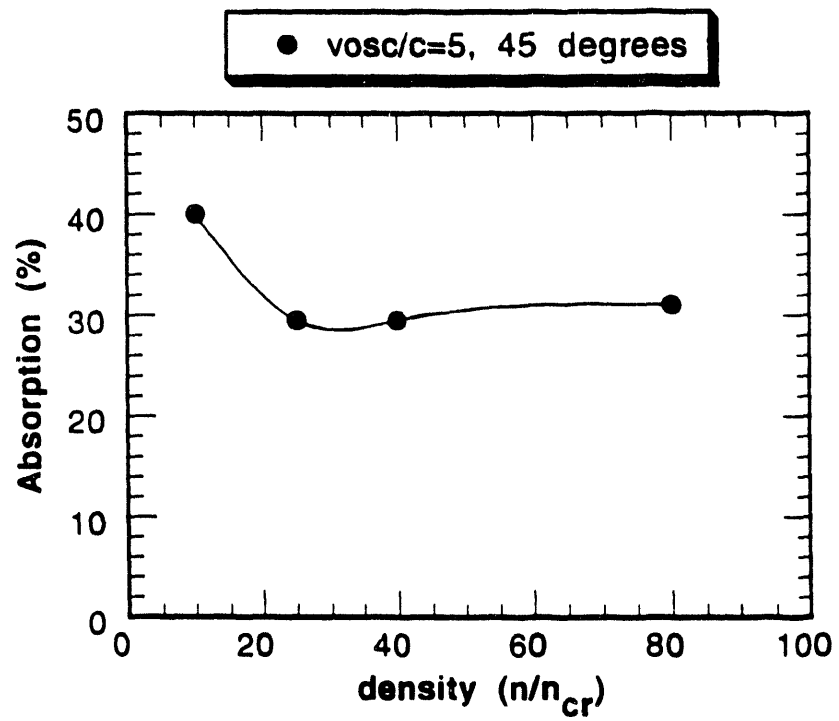


FIG. 3

DATE

FILMED

9 / 12 / 94

END

